THE JOURNAL OF PHYSICAL CHEMISTRY B

ARTICLE

pubs.acs.org/JPCB

Interactions within a [Ionic Liquid + Poly(ethylene glycol)] Mixture Revealed by Temperature-Dependent Synergistic Dynamic Viscosity and Probe-Reported Microviscosity

Shruti Trivedi and Siddharth Pandey*

Department of Chemistry, Indian Institute of Technology, Delhi, Hauz Khas, New Delhi 110016, India

Supporting Information

ABSTRACT: Mixtures of ionic liquid (IL) with poly(ethylene glycol) (PEG) may afford media with favorable properties. Dynamic viscosities of mixtures of a common and popular IL 1-butyl-3-methylimidazolium hexafluorophosphate ([bmim][PF_6]) with PEGs of average molecular weight (MW) 200 (PEG200), average MW 400 (PEG400), number-average MW M_n 570−630 (PEG600), and number-average MW M_n 950−1050 (PEG1000) over a complete composition range at 10° intervals in the temperature range of 10−90 °C are measured. The temperature dependence of the dynamic viscosity shows ([bmim][PF_6] + PEG) mixtures to behave as Newtonian fluids and is found to follow Arrhenius-type behavior. In the IL-rich region, excess logarithmic viscosities for the ([bmim][PF_6] + PEG200) mixture are found to be negative and independent of the temperature. Mixtures of ([bmim][PF_6] + PEG600) and ([bmim][PF_6] + PEG1000) show rare and unusual viscosity "synergism" or "hyperviscosity" in the sense that the mixture viscosity is observed to be significantly higher than the viscosity of both the neat components forming the mixture, giving rise to large positive excess logarithmic viscosities. These positive excess logarithmic viscosities decrease with increasing temperature. Formation of extensive H-bonding between the IL and PEG more than compensates for the losses in Coulombic attractive and van der Waals interactions within [bmim][PF_6] and PEG600/PEG1000, respectively, giving rise to viscosity synergism. This compensation is not enough for ([bmim][PF_6] + PEG200) and ([bmim][PF_6] + PEG400) mixtures. The evidence for H-bonding in the mixtures is provided by FTIR absorbance data. The product of the monomer-to-excimer emission intensity ratio and the lifetime of the intramolecular excimer fluorescence of a microfluidity probe, 1,3-bis(1-pyrenyl)propane (BPP), is used as a reflection of the microviscosity of the mixture at different temperatures. The microviscosity shows synergistic effects in all four ([bmim][PF_6] + PEG) mixtures. The contribution of H-bonding to the microviscosity reported by BPP is observed to be more then that as compared to contributions of Coulombic and van der Waals interactions. Synergism in the dynamic viscosity and microviscosity of ([bmim][PF_6] + PEG) mixtures is a complex interplay of inter- and intramolecular H-bonding as well as Coulombic and van der Waals type interactions.

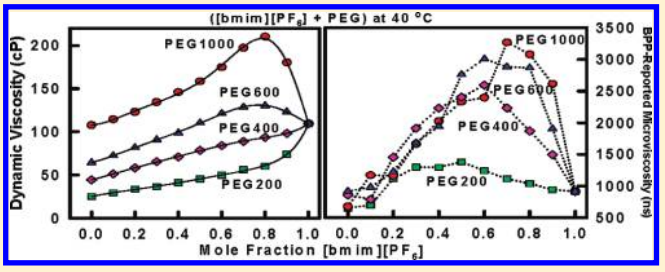

INTRODUCTION

The unique and interesting physicochemical properties of ionic liquids (ILs) have engrossed researchers throughout the world.[1] Due to their negligible vapor pressure, ILs have been recommended as potential green and environmentally benign replacements for conventional volatile organic compounds (VOCs).[2] A major reason for the increasing popularity of ILs as alternate solubilizing media is that ILs are constituted entirely of ions as opposed to the conventional molecular solvents usually used in chemistry. The possibility that a liquid constituted of ions alone may offer favorable and, in many cases, unusual outcomes is perhaps the most intriguing feature of ILs. Consequently, several applications and use of ILs in organic, inorganic, physical, materials, and biochemistry have been demonstrated during the past decade and a half.[3] Apart from reports on better performance of ILs in many of the applications, several of these investigations also reveal outcomes that are unexpected or unusual.[4] Many drawbacks, however, associated with ILs are also realized during these investigations. Among others, limited solubilizing capacity toward several common solutes and restricted physicochemical properties, especially viscosity, are perhaps the most noteworthy. Presently, they are the cause of major concern to the scientific community promoting ILs. It is worthwhile to mention that more than a decade after the rediscovery of these substances, the cost of preparation and purification of ILs is still quite high.

Cosolvent-modified ILs may alleviate the problem of limited solute solubility associated with many ILs as well as provide easily affordable solubilizing media with favorably modified physicochemical properties. This approach has the potential to increase

Received: April 2, 2011
Revised: May 2, 2011
Published: May 17, 2011

the utility and applications of ILs many-fold. Recognizing this, researchers, including us, have started exploring properties and application potentials of cosolvent-modified IL systems.[4d,e,5] In line with the potential environmentally benign aspect of ILs, understandably, the most relevant choices take into account the toxicity of the cosolvent selected. Subsequently, greener alternatives, such as, water,[6] sc CO_2,[7] ethanol,[8] renewable solvents,[9] liquid polymers,[10] and so forth become obvious choices as cosolvents to form potentially hybrid green media with ILs. Among these alternatives, poly(ethylene glycols) (PEGs) and related compounds have become cosolvents of major importance due to their interesting properties that may be varied vastly by simply varying the average molecular weight (MW) of the polymer.[11] PEGs have found immense industrial, pharmaceutical, and biomedical importance due, in major part, to their environmentally benign nature.[10b,11] It is hypothesized that due to the presence of an array of interactions stemming from the molecular architectures of ILs and PEGs, mixing an IL with a PEG may result in a medium that possesses interesting and favorable physicochemical properties. In retrospect, properties of a PEG may also get modified in favorable manner by addition of an IL to it.

We have measured dynamic viscosities of mixtures of a common and popular IL 1-butyl-3-methylimidazolium hexafluorophosphate ([bmim][PF_6]) with PEGs of average MW 200 (PEG200), average MW 400 (PEG400), number-average MW M_n 570−630 (PEG600), and number-average MW M_n 950−1050 (PEG1000) over a complete composition range at 10° intervals in the temperature range of 10−90 °C. Viscosity, as a function of temperature, is perhaps the most important property that will govern the use of ([bmim][PF_6] + PEG) mixtures in most industrial, pharmaceutical, chemical, and biotechnological applications. Furthermore, viscosity is an essential parameter that helps develop any solubilizing milieu and plays a major part in chemical transformations in solution.[12] During our assessment of the interactions present within ([bmim][PF_6] + PEG) mixtures through the analysis of the bulk viscosity data, we encountered a rare viscosity synergism or hyperviscosity. Specifically, for ([bmim][PF_6] + PEG1000) and ([bmim][PF_6] + PEG600), the viscosity of the mixture was found to be higher than the viscosity of either of the two neat components. In order to gain further insight into this rare and unusual hyperviscosity, we measured the microviscosity of ([bmim][PF_6] + PEG) mixtures at various temperatures using a common and popular fluorescence microfluidity probe, 1,3-bis(1-pyrenyl)propane (BPP). The microviscosity was taken as the product of the fluorescence lifetime of the intramolecular excimer (τ_E) and the ratio of monomer-to-excimer emission intensities (I_M/I_E) of BPP.[13] Though the importance of bulk viscosity in many industrial and academic setups is obvious, microviscosity pertaining to information about the viscosity sensed by a solute within the solubilizing milieu has immense importance in chemistry. Depending on the extent and type of solute−solvent interactions within the cybotactic region of the solute, there may or may not exist a correlation between the microviscosity reported by a probe and the bulk viscosity measured experimentally.[13a] In many instances in chemistry, the viscosity sensed by a solute, that is, the microviscosity, is of more importance in comparison to the bulk viscosity of the solution. We found that the microviscosity reported by BPP shows significant synergism in all four ([bmim][PF_6] + PEG) mixtures. Furthermore, important information regarding various types of interactions within ([bmim][PF_6] + PEG) mixtures is obtained from temperature dependence of the bulk viscosity as well as the microviscosity. Composition- and temperature-dependent contributions from H-bonding, Coulombic attractive and van der Waals type interactions toward bulk viscosity and microviscosity lead to the observed viscosity synergism within ([bmim][PF_6] + PEG) mixtures.

EXPERIMENTAL SECTION

Materials. BPP was obtained from Molecular Probes and was used as received. PEG200, PEG400, PEG600, and PEG1000 were obtained in highest purity from Sigma-Aldrich Co. and stored under dried conditions. IL [bmim][PF_6] was obtained from Merck (Ultrapure, halide content < 100 ppm; water content < 100 ppm) and was stored under dry argon.

Methods. The stock solution of BPP was prepared in ethanol and stored in an amber glass vial at 4 ± 1 °C. The required amount of BPP to prepare the stock solution was weighed using a Mettler−Toledo AB104-S balance with a precision of ±0.1 mg. The ([bmim][PF_6] + PEG) mixtures were prepared by mass using a Denver Instrument balance having a precision of ±0.1 mg. PEG1000 is solid at ambient conditions with a melting point of ∼38 °C. Therefore, the solutions for PEG1000 were prepared by melting it in a water bath at ∼60 °C and then mixing it with appropriate aliquots of [bmim][PF_6]. This system was allowed to equilibrate to the desired temperature before any data acquisition. An appropriate amount of BPP solution from the stock was transferred to a glass vial. The ethanol was evaporated with a gentle stream of high-purity nitrogen gas. [bmim][PF_6], PEG, or an appropriate ([bmim][PF_6] + PEG) mixture was added to achieve the desired final concentration of the probe.

In order to obtain dynamic viscosities (η), the earlier reported required density values were measured using a Mettler−Toledo DE45 delta range density meter.[14] The η were measured with a Peltier-based (resolution of 0.01 °C and accuracy < 0.05 °C) automated Anton Paar Micro Viscometer having calibrated glass capillaries of different diameters (1.6, 1.8, 3.0, and 4.0 mm). This instrument is based on the rolling ball principle, where the steel ball rolls down the inside of inclined, sample-filled calibrated glass capillaries. The deviation in η was ≤0.5%. Fluorescence spectra were acquired on model FL 3-11, Fluorolog-3 modular spectrofluorometer with single Czerny−Turner grating excitation and emission monochromators having a 450 W Xe arc lamp as the excitation source and PMT as the detector purchased from Horiba−Jobin Yvon, Inc. The temperature was controlled with a Thermo NESLAB RTE7 circulating chiller bath having a stability of ±0.01 °C. All data were acquired using 1 cm path length quartz cuvettes. The spectral response from appropriate blanks was subtracted before data analysis. Data analysis was performed by SigmaPlot v10 software. In order to obtain τ_E, excited-state fluorescence intensity decay data were acquired in the time domain using a Horiba−Jobin Yvon Fluorocube time-correlated single photon counting (TCSPC) fluorimeter. The BPP dissolved in ([bmim][PF_6] + PEG) mixtures at different temperatures were excited at 340 nm using a UV-pulsed NanoLED-340 source having a pulse width < 1.0 ns. The emission was collected using a Peltier-cooled red-sensitive TBX-04 PMT detection module at 487 nm. The temperature was controlled with a Peltier (TC 125) having an accuracy of ±0.3 °C and a stability of ±0.03 °C. The data were collected with a DAQ-MCA-3 Series

Table 1. Dynamic Viscosity, η (cP), of ([bmim][PF_6] + [PEG]) Mixtures at Different Temperatures (T)[a]

[bmim][PF_6]		T (°C)								
wt%	(mole frac.)	10	20	30	40	50	60	70	80	90
				[bmim][PF_6] + PEG200						
0.00	(0.0)	116.02	63.96	38.72	25.22	17.41	12.28	9.14	7.02	5.53
13.74	(0.1)	159.14	83.66	47.25	29.58	19.73	13.87	10.18	7.74	6.05
25.91	(0.2)	194.12	96.88	54.38	33.68	22.14	15.52	11.41	8.68	6.77
37.81	(0.3)	232.55	109.98	60.66	36.62	23.98	16.69	12.20	9.25	7.23
48.66	(0.4)	262.32	123.60	67.34	41.21	26.82	18.50	13.31	10.02	7.68
58.69	(0.5)	291.81	138.53	75.27	45.38	29.59	20.65	14.29	10.77	8.37
68.09	(0.6)	325.63	152.14	82.58	49.81	32.24	22.20	15.56	11.71	9.08
76.86	(0.7)	367.64	171.89	93.44	56.26	36.63	25.34	17.30	13.13	10.29
80.00	(0.8)	438.49	184.24	99.89	60.03	38.99	26.86	18.70	14.15	12.28
92.56	(0.9)	542.41	223.28	125.32	74.15	48.35	33.36	24.26	19.12	14.69
100.00	(1.0)	779.48	345.06	185.07	109.64	69.70	46.59	32.67	23.85	18.03
				[bmim][PF_6] + PEG400						
0.00	(0.0)	220.14	115.95	69.62	44.40	30.39	21.74	16.11	12.24	9.62
07.32	(0.1)	284.24	146.78	81.58	51.35	34.19	24.14	17.77	13.48	10.45
15.08	(0.2)	351.91	173.44	94.46	58.25	38.14	26.58	19.34	14.47	11.22
23.36	(0.3)	434.02	205.63	108.78	65.46	41.95	28.67	20.56	15.25	11.74
32.14	(0.4)	537.38	239.84	124.66	71.10	45.21	30.46	21.89	16.26	12.39
41.53	(0.5)	636.25	275.08	139.74	78.50	48.66	32.46	23.02	17.02	12.93
51.60	(0.6)	705.06	303.24	152.06	84.15	52.95	35.02	24.57	18.01	13.60
62.38	(0.7)	741.93	319.80	160.34	88.97	55.09	36.41	25.59	18.79	14.24
73.97	(0.8)	750.21	333.82	167.73	93.62	58.46	38.76	27.26	20.02	15.12
86.47	(0.9)	732.12	335.76	173.27	98.23	59.24	39.76	28.14	20.84	15.92
100.00	(1.0)	779.48	345.06	185.07	109.64	69.70	46.59	32.67	23.85	18.03
				[bmim][PF_6] + PEG600						
0.00	(0.0)	solid	solid	101.68	64.48	43.82	31.41	23.57	18.09	14.23
05.04	(0.1)	solid	203.35	116.32	72.42	48.47	34.06	25.00	19.11	14.98
10.61	(0.2)	solid	245.53	134.11	81.87	52.78	36.60	26.70	20.19	15.73
16.88	(0.3)	solid	285.34	151.95	90.97	58.22	39.65	28.52	21.41	16.57
24.00	(0.4)	solid	328.76	171.41	98.85	62.53	42.46	30.22	22.48	17.30
32.15	(0.5)	893.16	391.90	196.02	110.34	67.39	44.99	31.73	23.37	17.83
41.54	(0.6)	1068.77	452.67	218.27	121.40	72.54	47.94	33.30	24.38	18.48
52.48	(0.7)	1202.26	502.11	236.50	128.70	76.32	50.02	34.55	25.29	18.92
65.46	(0.8)	1200.13	504.64	239.78	130.35	77.44	50.48	34.70	25.18	18.98
80.84	(0.9)	1019.57	448.25	222.41	123.14	74.48	49.39	34.26	24.99	18.89
100.00	(1.0)	779.48	345.06	185.07	109.64	69.70	46.59	32.67	23.85	18.03
				[bmim][PF_6] + PEG1000						
0.00	(0.0)	soild	solid	solid	107.83	70.89	50.13	37.22	28.68	22.79
03.06	(0.1)	solid	solid	solid	114.51	76.14	53.36	39.22	29.74	23.51
06.63	(0.2)	solid	solid	solid	123.03	80.82	56.26	41.10	30.98	24.39
10.88	(0.3)	solid	solid	solid	134.49	87.69	60.08	43.25	31.97	24.92
15.93	(0.4)	solid	solid	solid	146.00	93.37	63.41	45.64	33.50	26.09
22.13	(0.5)	solid	solid	solid	158.43	98.36	65.89	46.21	34.29	26.50
29.90	(0.6)	solid	solid	320.51	174.99	107.48	70.80	49.11	36.09	27.38
39.87	(0.7)	solid	solid	367.33	197.31	116.89	75.83	51.05	37.47	28.07
53.19	(0.8)	solid	830.74	391.93	210.30	121.51	76.73	51.78	37.90	28.11
71.89	(0.9)	1725.14	721.74	341.32	180.31	103.16	66.34	45.83	33.24	24.80
100.00	(1.0)	779.48	345.06	185.07	109.64	69.70	46.59	32.67	23.85	18.03

[a] The error in η is $\leq$0.5%.

dx.doi.org/10.1021/jp203079p |J. Phys. Chem. B 2011, 115, 7405–7416

(P7882) multichannel analyzer. The excited-state fluorescence intensity decays were analyzed using DAS6 analysis software and were fitted to a biexponential decay from which τ_E were obtained.[13a] Fourier-transform infrared (FTIR) absorbance data were acquired from 4000 to 400 cm^{-1} on a Nicolet 6700 FTIR double-beam spectrophotometer. The liquid samples were evenly spread on KBr pellets to record the FTIR spectra.

RESULTS AND DISCUSSION

Temperature Dependence of the Dynamic Viscosity of ([bmim][PF_6] + PEG) Mixtures. Experimentally measured dynamic viscosities (η) of four ([bmim][PF_6] + PEG) mixtures over a complete composition range at 10° intervals in the temperature range of 10−90 °C are reported in Table 1. It is evident from the entries in Table 1 that, as expected, a monotonic decrease in η is observed as the temperature is increased from 10 to 90 °C for a ([bmim][PF_6] + PEG) mixture of a fixed composition. Further, at a given temperature and composition, η of the ([bmim][PF_6] + PEG) mixture is found to be higher for higher PEG average MWs. This is in line with the fact that η of neat PEG increases with an increase in the average MW of the PEG.[15] It is important to mention that η of neat [bmim][PF_6] and that of neat PEGs at various temperatures measured by us are in good agreement with those reported in the literature.[15,16]

The dependence of the viscosity of liquids on temperature has been studied by many researchers.[15,17] The de Guzman−Andrade empirical equation

$$\ln \eta = \ln \eta_0 + \frac{E_{a,\eta}}{RT} \quad (1)$$

is most used for Newtonian fluids in a limited temperature range.[18] This equation is based on the assumption that the fluid flow obeys the Arrhenius equation for molecular kinetics, where T is temperature in K, η_0 is a coefficient, $E_{a,\eta}$ is the activation energy of the viscous flow, and R is the universal gas constant. It is usually obeyed by first-order fluids. A first-order fluid is another name for a power law fluid with exponential dependence of viscosity on temperature. The de Guzman−Andrade equation is quite widely accepted as a fundamental relationship, and several theoretical or quasi-theoretical treatments have been advanced, leading to this form of equation.[18b] Plots of ln η versus $1/T$ along with the best-fit straight lines for the four ([bmim][PF_6] + PEG) mixtures are presented in Figure S1 (Supporting Information). Goodness-of-fit in terms of r^2 along with the recovered parameters are presented in Table 2. From a careful examination of the plots in Figure S1 (Supporting Information) and entries in Table 2, it may be inferred that ([bmim][PF_6] + PEG) mixtures behave similar to Newtonian fluids in the temperature range of 10−90 °C.

It is interesting to note that, among the four neat liquids, parameter η_0, representing η in the limit of $T \rightarrow \infty$, has the lowest value in [bmim][PF_6] and increases in the order [bmim][PF_6] < PEG200 < PEG400 < PEG600 < PEG1000. While this trend in η_0 of neat PEGs is the same as that shown by η of neat PEGs, η of neat [bmim][PF_6] does not follow the trend in η_0, that is, the η of neat [bmim][PF_6] is not the lowest of the four liquids (Table 1). This important outcome hints at the vast differences in the inter- as well as intramolecular interactions present in PEGs as opposed to those present in IL [bmim][PF_6]. This may highlight the Coulombic interaction as the predominant interaction within [bmim][PF_6] as opposed to the H-bonding and

Table 2. Results of linear Regression Analysis of the Temperature Dependence of Dynamic Viscosity (η) of ([bmim][PF_6] + PEG) Mixtures According to the Equation $\ln \eta = \ln \eta_0 + (E_{a,\eta}/RT)$ (eq 1)

wt% [bmim][PF_6]	($X_{[bmim][PF_6]}$)	ln η_0	$E_{a,\eta}$ (kJ·mol^{-1})	r^2
		[bmim][PF_6] + PEG200		
0.00	(0.0)	−9.1 (±0.4)	32.2 (±0.9)	0.9942
13.74	(0.1)	−9.8 (±0.4)	34.6 (±1.2)	0.9916
25.91	(0.2)	−10.0 (±0.5)	35.4 (±1.4)	0.9898
37.81	(0.3)	−10.3 (±0.6)	36.5 (±1.5)	0.9876
48.66	(0.4)	−10.4 (±0.6)	37.0 (±1.4)	0.9893
58.69	(0.5)	−10.4 (±0.5)	37.4 (±1.4)	0.9901
68.09	(0.6)	−10.4 (±0.6)	37.7 (±1.5)	0.9896
76.86	(0.7)	−10.3 (±0.5)	37.7 (±1.5)	0.9898
80.00	(0.8)	−10.3 (±0.7)	37.8 (±2.0)	0.9811
92.56	(0.9)	−10.0 (±0.7)	37.4 (±1.9)	0.9815
100.00	(1.0)	−10.3 (±0.6)	39.5 (±1.5)	0.9903
		[bmim][PF_6] + PEG400		
0.00	(0.0)	−8.8 (±0.4)	33.0 (±1.1)	0.9927
07.32	(0.1)	−9.3 (±0.5)	34.8 (±1.3)	0.9908
15.08	(0.2)	−9.8 (±0.5)	36.3 (±1.4)	0.9900
23.36	(0.3)	−10.3 (±0.6)	38.0 (±1.5)	0.9894
32.14	(0.4)	−10.8 (±0.6)	39.6 (±1.7)	0.9869
41.53	(0.5)	−11.2 (±0.7)	41.0 (±1.8)	0.9864
51.60	(0.6)	−11.3 (±0.7)	41.5 (±1.8)	0.9868
62.38	(0.7)	−11.3 (±0.7)	41.6 (±1.8)	0.9869
73.97	(0.8)	−11.1 (±0.6)	41.2 (±1.7)	0.9879
86.47	(0.9)	−10.9 (±0.6)	40.6 (±1.6)	0.9887
100.00	(1.0)	−10.3 (±0.6)	39.5 (±1.5)	0.9903
		[bmim][PF_6] + PEG600		
0.00	(0.0)	−7.3 (±0.3)	29.8 (±0.8)	0.9961
05.04	(0.1)	−8.2 (±0.4)	32.7 (±1.1)	0.9937
10.61	(0.2)	−8.8 (±0.5)	34.4 (±1.2)	0.9923
16.88	(0.3)	−9.1 (±0.5)	35.7 (±1.3)	0.9922
24.00	(0.4)	−9.5 (±0.5)	36.9 (±1.4)	0.9912
32.15	(0.5)	−11.0 (±0.7)	41.3 (±1.8)	0.9869
41.54	(0.6)	−11.5 (±0.7)	42.8 (±1.9)	0.9861
52.48	(0.7)	−11.8 (±0.8)	43.8 (±2.0)	0.9857
65.46	(0.8)	−11.8 (±0.7)	43.8 (±1.9)	0.9867
80.84	(0.9)	−11.2 (±0.7)	42.2 (±1.7)	0.9881
100.00	(1.0)	−10.3 (±0.6)	39.5 (±1.5)	0.9903
		[bmim][PF_6] + PEG1000		
0.00	(0.0)	−6.6 (±0.4)	29.2 (±1.0)	0.9955
03.06	(0.1)	−6.8 (±0.3)	29.9 (±0.8)	0.9970
06.63	(0.2)	−7.0 (±0.3)	30.6 (±0.8)	0.9969
10.88	(0.3)	−7.4 (±0.3)	31.9 (±0.8)	0.9975
15.93	(0.4)	−7.6 (±0.3)	32.6 (±0.9)	0.9969
22.13	(0.5)	−8.0 (±0.4)	33.8 (±1.1)	0.9955
29.90	(0.6)	−9.1 (±0.5)	37.2 (±1.4)	0.9930
39.87	(0.7)	−9.7 (±0.5)	39.0 (±1.5)	0.9928
53.19	(0.8)	−10.9 (±0.6)	42.6 (±1.7)	0.9902
71.89	(0.9)	−11.9 (±0.7)	45.0 (±2.0)	0.9867
100.00	(1.0)	−10.3 (±0.6)	39.5 (±1.5)	0.9903

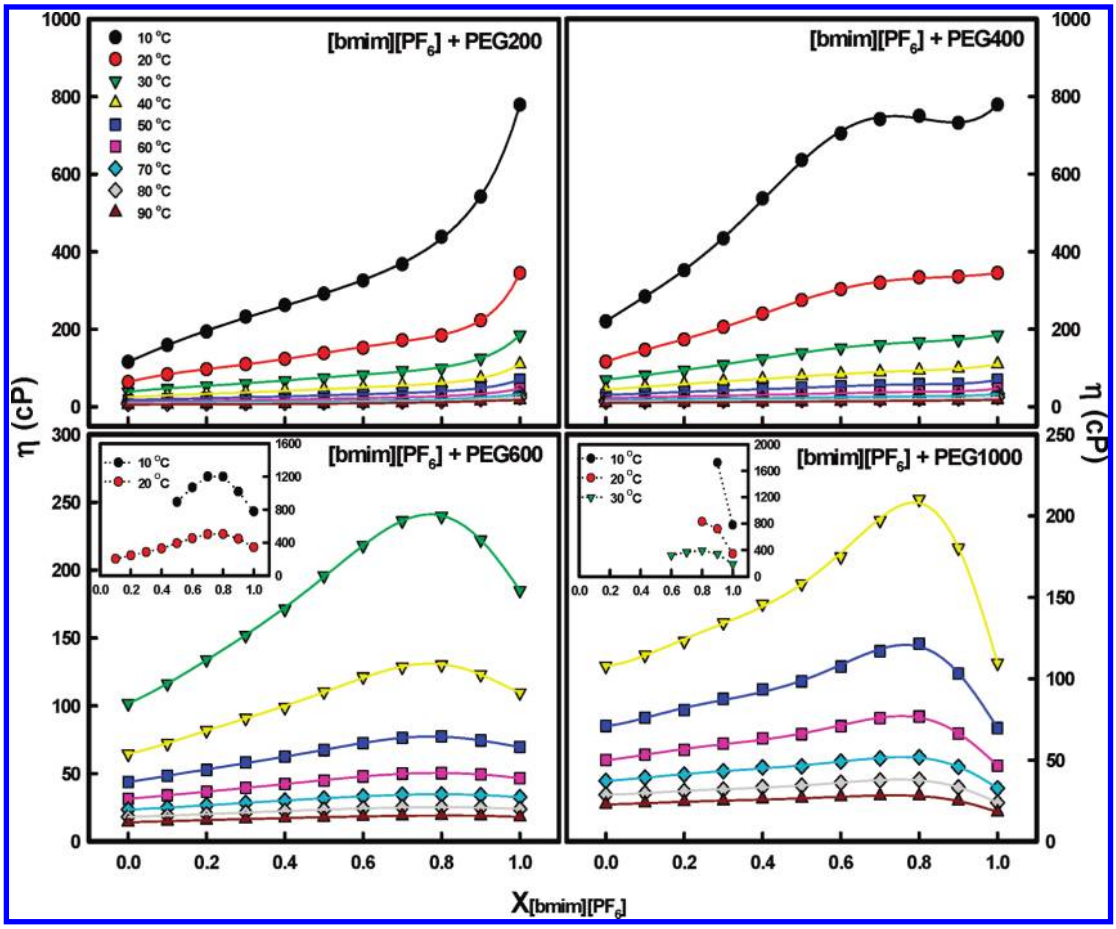

Figure 1. Dynamic viscosity (η) as a function of [bmim][PF_6] mole fraction ($X_{[bmim][PF_6]}$) for ([bmim][PF_6] + PEG) mixtures at different temperatures. Solid curves at each temperature are obtained using the best fit parameters of the Redlich−Kister polynomial (eq 3) reported in Table 3. The error in measured η is ≤0.5%.

van der Waals type interactions to be the major interactions within PEGs. $E_{a,\eta}$ in neat [bmim][PF_6] and PEGs further support this observation as $E_{a,\eta}$ is significantly higher for [bmim][PF_6] as compared to those for neat PEGs. The $E_{a,\eta}$ appears to increase, in general, with the concentration of [bmim][PF_6] in the mixture before attaining its value in neat IL [bmim][PF_6]. However, it is interesting to note that, except for mixtures with PEG200, at certain compositions of ([bmim][PF_6] + PEG) mixtures (mostly in the IL-rich region), $E_{a,\eta}$ becomes higher than that observed in neat [bmim][PF_6]. Similarly, η_0 becomes lower than that found for neat [bmim][PF_6] at similar compositions in the IL-rich region. These key outcomes are manifested in the viscosity synergism or hyperviscosity observed for [bmim][PF_6] mixtures with PEG600 and PEG1000, respectively (vide infra).

Composition Dependence of Dynamic Viscosity of ([bmim][PF_6] + PEG) Mixtures. Plots of η versus $X_{[bmim][PF_6]}$ (mole fraction of [bmim][PF_6], calculated using the average MW of PEG) for ([bmim][PF_6] + PEG) mixtures at different temperatures show interesting and unusual trends (Figure 1). Within the ([bmim][PF_6] + PEG200) mixture at fixed temperature, η increases monotonically upon increasing $X_{[bmim][PF_6]}$. This is expected as η of neat [bmim][PF_6] is significantly higher than the η of neat PEG200 at all investigated temperatures. Similar observations were reported earlier for the ([bmim][PF_6] + TEG) mixture at ambient temperature.[4d] The trend in increase in η with increasing $X_{[bmim][PF_6]}$ changes considerably for the ([bmim][PF_6] + PEG400) mixture, especially in the IL-rich region, where the increase in η with $X_{[bmim][PF_6]}$ is not as dramatic as that observed within the ([bmim][PF_6] + PEG200) mixture. The η even decreases in going from $X_{[bmim][PF_6]} \approx 0.8$ to 0.9 before increasing to its value in neat [bmim][PF_6] at 10 °C. As the difference between η of the two neat components decreases considerably ($\eta_{[bmim][PF6]}$ versus η_{PEG600}) and becomes comparable ($\eta_{[bmim][PF6]}$ versus $\eta_{PEG1000}$), the η of the mixture becomes highly unusual. Specifically, η of the mixture increases and attains a maxima before decreasing again; the maximum η in most cases is observed at $X_{[bmim][PF_6]} \approx 0.8$, irrespective of the temperature of the mixture. The most unusual outcome is the synergistic aspect of η observed within ([bmim][PF_6] + PEG600) and ([bmim][PF_6] + PEG1000) mixtures, where η of the mixture is found to be even higher than that of the more viscous of the two neat components. The observation, which is similar to the hyperpolarity observed earlier for ([bmim][PF_6] + PEG) and ([bmim][PF_6] + TEG) mixtures,[4d,e] is rather rare and unusual and is termed hyperviscosity.

Excess Logarithmic Viscosity and Redlich−Kister Treatment. In order to assess the interactions within ([bmim][PF_6] + PEG) mixtures, excess logarithmic viscosities, $(\ln \eta)^E$, of ([bmim][PF_6] + PEG) mixtures were calculated from the

dx.doi.org/10.1021/jp203079p |J. Phys. Chem. B 2011, 115, 7405–7416

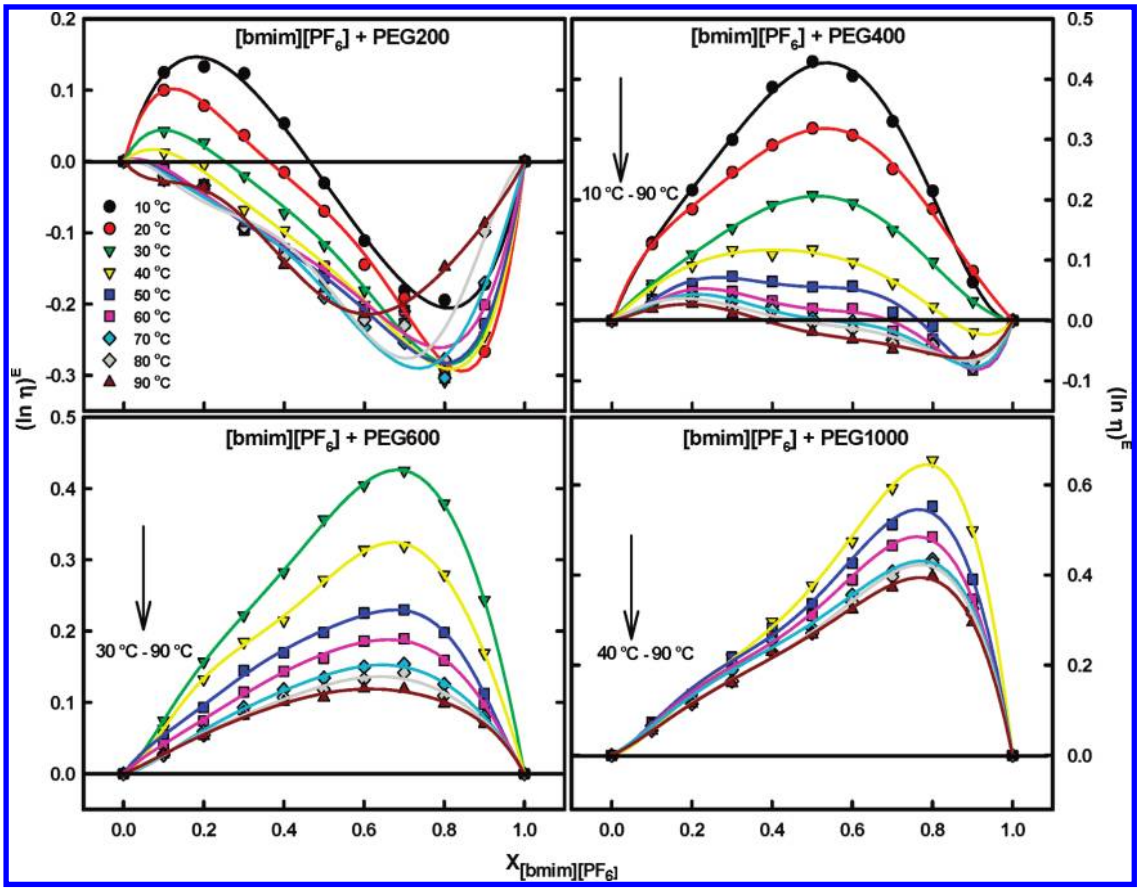

Figure 2. $(\ln \eta)^E$ versus $X_{[\mathrm{bmim}][\mathrm{PF}_6]}$ for ([bmim][PF_6] + PEG) mixtures at different temperatures. Solid curves at each temperature are obtained using the best fit parameters of the Redlich−Kister polynomial (eq 3) reported in Table 3.

equation[19]

$$(\ln \eta)^E = \ln \eta - [X_{[\mathrm{bmim}][\mathrm{PF}_6]} \ln \eta_{[\mathrm{bmim}][\mathrm{PF}_6]} + X_{\mathrm{PEG}} \ln \eta_{\mathrm{PEG}}] \quad (2)$$

Plots of $(\ln \eta)^E$ versus $X_{[\mathrm{bmim}][\mathrm{PF}_6]}$ for all four ([bmim][PF_6] + PEG) mixtures in the temperature range of 10−90 °C are presented in Figure 2. Positive deviations at all temperatures over the entire composition range are clearly observed for ([bmim][PF_6] + PEG600) and ([bmim][PF_6] + PEG1000) mixtures; importantly, the $(\ln \eta)^E$ decreases with increasing temperature. However, the deviations are observed to become slightly negative for ([bmim][PF_6] + PEG400) mixtures; the higher the temperature, the lower the $X_{[\mathrm{bmim}][\mathrm{PF}_6]}$ at which $(\ln \eta)^E$ becomes 0. On the contrary, the deviations are significantly negative for ([bmim][PF_6] + PEG200) mixtures; at $T > 40$ °C, $(\ln \eta)^E$ are observed to be negative at all compositions of the mixture. The higher the temperature, the lower the $X_{[\mathrm{bmim}][\mathrm{PF}_6]}$ at which $(\ln \eta)^E$ becomes 0, which is observed for $10 \leq T \leq 40$ °C nonetheless. It is noteworthy that while positive $(\ln \eta)^E$ is observed to decrease with increasing T, no such trend in negative $(\ln \eta)^E$ with T is observed. This T dependence hints at H-bonding as being the possible interaction when $(\ln \eta)^E$ is positive and the loss of Coulombic attraction as being the major reason for negative $(\ln \eta)^E$ (vide infra).

The $(\ln \eta)^E$ or the excess viscosity, η^E, was reported for many IL-containing mixtures before, and both negative and positive deviations were observed, depending on the IL as well as the cosolvent.[20] In one of the relevant investigations, imidazolium ILs, [emim][BF_4], [bmim][BF_4], [emim][OTf], and [bmim][OTf], were demonstrated to exhibit positive $(\ln \eta)^E$ when mixed with poly(ethylene glycol)dimethacrylate (PEG DMA) and poly(ethylene glycol)monomethacrylate (PEG MMA) at 40 °C.[20a] IL [bmim][PF_6] showed positive $(\ln \eta)^E$ when mixed with acetone, 2-butanone, 3-pentanone, cyclopentanone, and ethyl acetate,[20b] and [bmim][BF_4] showed mostly positive (negative at few compositions) $(\ln \eta)^E$ when mixed with acetonitrile, dichloromethane, 2-butanone, and DMF.[20c] However, [bmim][BF_4] mixtures with methyl formate, ethyl formate, methyl acetate, and acetone[20d] and [bmim][NO_3][20e] and [omim][NO_3][20f] mixtures with ethanol, 1-propanol, and 1-butanol surprisingly exhibit negative η^E. Among pyridinium ILs, while the [4-methyl-*N*-butylpyridinium][BF_4] mixture with methanol shows positive $(\ln \eta)^E$,[20g] [1-butylpyridinium][BF_4] and [1-octylpyridinium][BF_4] mixtures with water exhibit negative η^E.[20h] While a mixture of pyrrolidinium octanoate with water shows positive η^E, the mixtures of the same IL with methanol, ethanol, *n*-butanol, and acetonitrile show negative η^E.[20i]

Our $(\ln \eta)^E$ were also correlated by the Redlich−Kister polynomial equation.[21] According to the combined nearly ideal binary solvent/Redlich−Kister (CNIBS/R-K) model, the $(\ln \eta)^E$ in a binary mixture at a constant temperature can be expressed as

$$(\ln \eta)^E = X_{[\mathrm{bmim}][\mathrm{PF}_6]} X_{\mathrm{PEG}} \sum_{j=0}^{k} A_j (X_{[\mathrm{bmim}][\mathrm{PF}_6]} - X_{\mathrm{PEG}})^j \quad (3)$$

Table 3. Parameters (A_j) and Correlation Coefficient (r^2) Recovered from the Best Fit of $(\ln \eta)^E$ according to the Redlich−Kister Polynomial (eq 3) for ([bmim][PF$_6$] + PEG) Mixtures

T/°C	A_0	A_1	A_2	A_3	A_4	r^2
			[bmim][PF$_6$] + PEG200			
10	−0.1149	−1.5673	−0.1527	−0.7267	−0.1260	0.9979
20	−0.2728	−1.0677	−0.9164	−2.3143	−0.1835	0.9987
30	−0.4590	−1.1141	−1.0685	−1.3058	0.1774	0.9950
40	−0.5736	−0.9448	−0.9734	−1.3612	−0.2330	0.9946
50	−0.6455	−0.8489	−1.0607	−1.0455	−0.0518	0.9909
60	−0.6101	−0.8115	−1.0527	−0.8543	0.2363	0.9848
70	−0.7185	−1.2422	−1.1705	0.2202	0.9762	0.9754
80	−0.6809	−1.3480	−1.4079	1.1759	2.1376	0.9090
90	−0.7653	−0.8066	0.7908	0.6233	−0.9145	0.9889
			[bmim][PF$_6$] + PEG400			
10	1.6941	0.4157	−1.0921	−1.3339	0.1974	0.9897
20	1.2657	0.2398	−0.5433	−0.8391	0.5916	0.9618
30	0.8244	0.0649	−0.5815	−0.4084	0.1584	0.9936
40	0.4496	−0.1928	−0.0949	−0.5014	−0.4678	0.9950
50	0.2236	−0.0541	0.3944	−1.1232	−1.7586	0.9883
60	0.0768	−0.1372	0.4511	−0.9662	−1.6052	0.9903
70	0.0129	−0.1808	0.3786	−0.8442	−1.3056	0.9900
80	−0.0168	−0.1842	−0.1914	−0.7500	−0.7620	0.9888
90	−0.0807	−0.2630	0.2454	−0.4588	−0.7472	0.9948
			[bmim][PF$_6$] + PEG600			
30	1.4067	1.2019	0.9433	−0.0552	−0.5874	0.9995
40	1.0756	0.8611	0.9105	−0.2068	−0.8986	0.9975
50	0.8055	0.6110	0.5088	−0.3065	−0.5038	0.9929
60	0.6720	0.4736	0.2466	−0.1240	−0.1425	0.9959
70	0.5503	0.3344	0.1710	0.0605	−0.1732	0.9966
80	0.4943	0.2892	0.1192	0.0535	−0.0324	0.9841
90	0.4506	0.1849	0.0496	0.1688	0.1404	0.9917
			[bmim][PF$_6$] + PEG1000			
40	1.4968	2.0426	2.7838	1.6367	−0.4385	0.9993
50	1.3623	1.7417	2.5374	0.7840	−1.0054	0.9976
60	1.2662	1.5020	2.1071	0.6920	−0.7465	0.9986
70	1.1736	1.1724	1.6430	1.0178	−0.1283	0.9985
80	1.0955	1.2713	1.7430	0.8412	−0.3945	0.9990
90	1.0752	1.1194	1.4347	0.8781	−0.1089	0.9988

where A_j and j are the equation coefficients and the degree of the polynomial expansion, respectively. The numerical values of j can be varied to find an accurate mathematical representation of the experimental data. Regression analysis was performed to fit the polynomials (eq 3) to our experimental data, and the results of the fit are reported in Table 3. The fitting parameters are highlighted by the positive A_j ($j \leq 3$) values for ([bmim][PF$_6$] + PEG1000) that start to become negative as the PEG average MW is decreased. It is observed from the r^2 values that the data show good fitting for all four ([bmim][PF$_6$] + PEG) mixtures at all temperatures. The solid curves connecting η and $(\ln \eta)^E$ in Figures 1 and 2, respectively, are obtained from the CNIBS/R-K model fit (with $j = 4$), as reported in Table 3, which further supports the good correlation between the predicted and the experimentally obtained values. It is convenient to use a cross-validation method, which is a practical and reliable method to test the predictive significance when only little data are available.[22]

Reasons for the Synergistic Dynamic Viscosity and Trends in $(\ln \eta)^E$. The unusually high η of ([bmim][PF$_6$] + PEG600) and ([bmim][PF$_6$] + PEG1000) mixtures is undoubtedly the most interesting aspect of our results. To re-emphasize, the η of these mixtures at several compositions and temperatures is observed to be even higher than that of the neat component having higher η of the two (Figure 1). This is a rarely observed phenomenon. As far as ILs are concerned, to the best of our knowledge, there exists only one report showing such viscosity synergism or hyperviscosity in mixtures of (IL + PEG DMA, with 9 ethoxy units in PEG) and (IL + PEG MMA, with 6.2 ethoxy units in PEG) at 40 °C for ILs [emim][BF$_4$] and [emim][OTf], respectively.[20a] The authors deemed the results surprising, albeit no explanation was offered. Non-IL systems that show such a synergistic viscosity effect under certain conditions are aqueous mixtures of hydroxypropyl-substituted guar and carboxymethyl hydroxypropyl-substituted guar,[23] short-chain alcohols,[24] acetone,[24b,25] dimethyl sulfoxide,[26] nitric acid,[27] and isobutyric acid.[28] Among very few nonaqueous mixtures demonstrating this hyperviscosity are (*o*-chlorophenol + dioxane),[29] (dimethyl sulfoxide + acetic acid),[29] (methanol + chloroform),[30] (methanol + toluene),[31] and (carbon tetrachloride + ethyl acetate).[31] It is amply evident that this synergistic viscosity effect is rather rare, especially for nonaqueous mixtures.

The large difference in the size and/or the shape of the component species of the mixture and the loss of Coulombic attractive interaction (or dipolar association) within the mixture as compared to that in the neat components usually result in decreased η of the mixture. Specific interactions between the two component species, for example, formation of H-bonds and charge-transfer complexes, on the other hand, increase the η of the mixture. Both the size and shape of IL [bmim][PF$_6$] are very different from the size and shape of PEG600 and PEG1000, and there certainly is the loss of Coulombic attractive interaction present within IL [bmim][PF$_6$] upon forming the ([bmim][PF$_6$] + PEG) mixture; the η of the mixture, on the contrary, is observed to be unusually high. For ([bmim][PF$_6$] + PEG) mixtures, the closer the η of the two neat components, the greater the synergism in η of the mixture. We hypothesize the extensive formation of H-bonds between IL [bmim][PF$_6$] and PEG600 or PEG1000 resulting in increased cohesive forces to be the main reason for the observed synergism in η of the mixture. The T dependence of $(\ln \eta)^E$ (vide supra) adequately supports our proposition as the positive $(\ln \eta)^E$ is observed to decrease with increasing T as the H-bond strength weakens at higher T.[32]

The possibility of H-bonding between the C2−H of the bmim$^+$ and −O− of the termini −OH and that between C2−H of the bmim$^+$ and −O− of the ethoxy units of PEG were documented in the literature earlier.[4d] The role of H-bonding between C2−H of the bmim$^+$ of the IL and −O− of the ethoxy units of PEG must also be evoked in observed viscosity synergism as greater the average MW of PEG, the greater the number of the ethoxy units, resulting in more H-bonding within the mixtures. H-bonding possibilities between PF_6^- of the IL and −H of the termini −OH of PEG may not be disregarded either. We believe that though H-bonding takes place in mixtures of [bmim][PF$_6$] with PEG200 and PEG400 it is not as extensive as in the case of [bmim][PF$_6$] mixtures of PEG600 and PEG1000 to overtake the losses in Coulombic attractive interactions within [bmim][PF$_6$]. Subsequently, hyperviscosity is not observed in

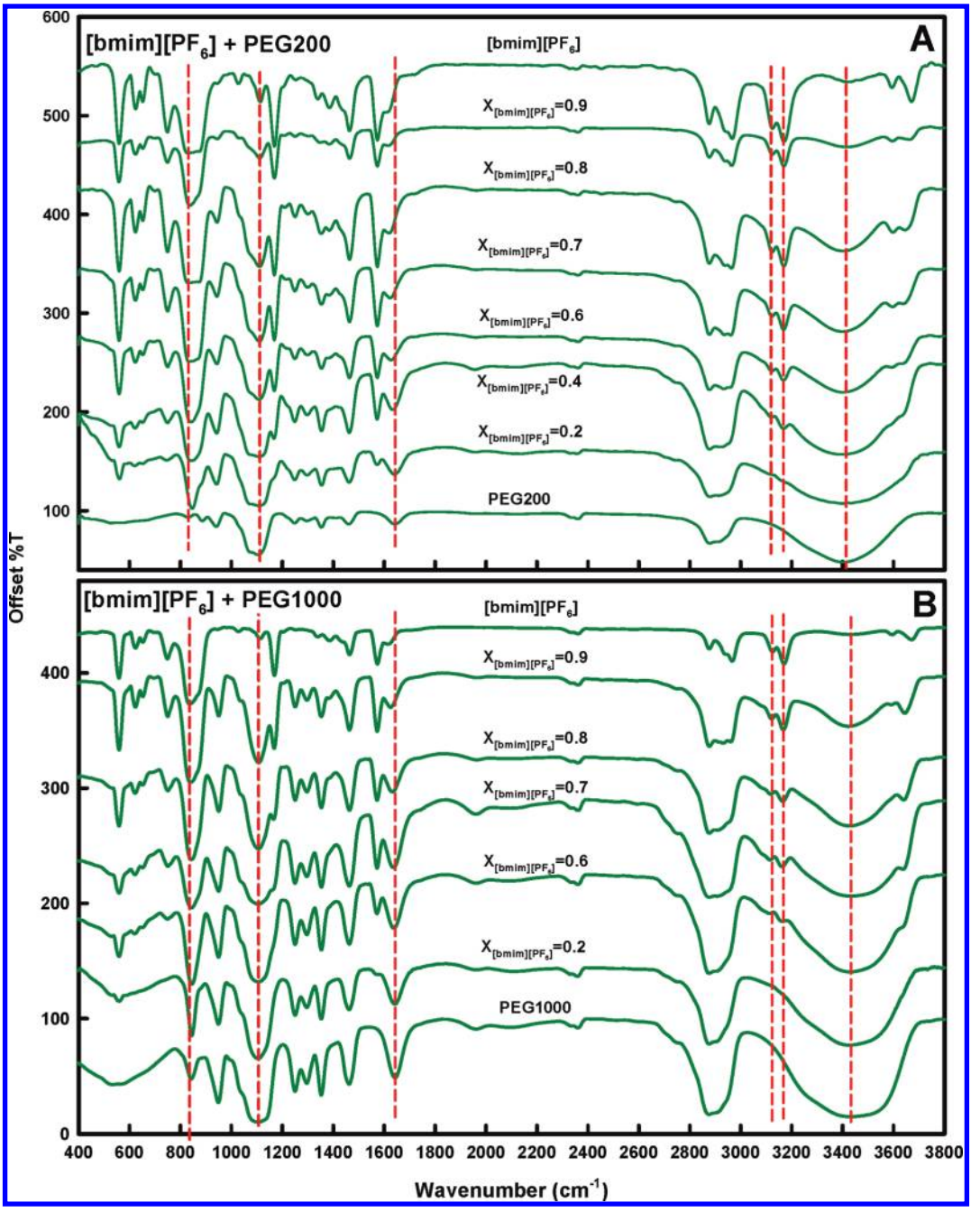

Figure 3. FTIR absorbance spectra of the ([bmim][PF_6] + PEG200) mixture (A) and the ([bmim][PF_6] + PEG1000) mixture (B) at ambient conditions. Dashed vertical lines illustrate the spectral shifts.

mixtures of ([bmim][PF_6] + PEG200) and ([bmim][PF_6] + PEG400) at any temperature. This hypothesis is well supported by the observation that $(\ln \eta)^E$ is found to be negative in the [bmim][PF_6]-rich region and becomes positive in the PEG-rich region for mixtures of PEG200 and PEG400 with [bmim][PF_6]. In the [bmim][PF_6]-rich region, the losses in columbic attraction could not be compensated for by the specific H-bonding interactions, and thus, η of the mixture is lower than that expected from ideal behavior. In further support of this, the negative $(\ln \eta)^E$ is observed to be almost independent of the temperature of the system.

The extensive H-bond formation between PEG and [bmim][PF_6] is further elucidated by FTIR absorption spectra (Figure 3) and IR absorbance peak assessments (Table S1, Supporting Information) of ([bmim][PF_6] + PEG200) and ([bmim][PF_6] + PEG1000) mixtures at ambient conditions. In the FTIR absorption spectrum of PEGs, usually the peaks in the vicinity of (3430−3400) and (1645−1640) cm^{-1} are attributed to the −OH bond, and the peak in the vicinity of (1105−1100) cm^{-1} is attributed to the −C−O− bond, whereas the peaks in the ranges (2877−2875), (1465−1460), and (1355−1350) cm^{-1} are responsible for the $-CH_2$ in the molecular chain.[33] A careful examination of the FTIR data reveals the maximum shift to lower wavenumbers for the peak in the vicinity of (1645−1640) cm^{-1} for PEG mixtures of

[bmim][PF_6]; for a mixture of ([bmim][PF_6] + PEG1000), the peak at 3429 cm^{-1} corresponding to the −OH bond of PEG1000 also shows significant lowering in wavenumbers as [bmim][PF_6] is added to PEG1000. Similarly, to our convenience, the peaks for [bmim][PF_6][34] corresponding to the −NC(H)N− bond at 829, 3124, and 3170 cm^{-1} show considerable shifts when PEG1000 is added to [bmim][PF_6]. For PEG200 addition, however, the shift is statistically meaningful for the peak appearing at 829 cm^{-1} only. It is also important to mention here that while peaks at 3124 and 3170 cm^{-1} shift to lower wavenumbers, the shift is to higher wavenumbers for the 829 cm^{-1} peak as PEG1000 is added to [bmim][PF_6]. This could be due to the fact that while 829 cm^{-1} is attributed to the −NC(H)N− bend, 3124 and 3170 cm^{-1} are assigned to the −NC(H)N− CH stretch.[34] The presence of H-bonding within mixtures of ([bmim][PF_6] + PEG) is clearly evident; however, the FTIR absorption data hint at H-bonding to be more extensive and stronger within the ([bmim][PF_6] + PEG1000) mixture as compared to that that within the ([bmim][PF_6] + PEG200) mixture. This may be the reason for the rare hyperviscosity or the synergistic bulk viscosity observed within [bmim][PF_6] mixtures with PEG600 and PEG1000.

Microviscosity of ([bmim][PF_6] + PEG) Mixtures from 1,3-Bis(1-pyrenyl)propane Fluorescence. The information on microviscosity (η_μ), the viscosity sensed by a solute in a solution, is of utmost importance in all areas of chemistry, including chemical reactions, extractions, chromatography, electrochemistry, spectroscopy, and more.[13a] In many instances, viscosity sensed by a solute has more relevance in chemistry as compared to the bulk viscosity, especially when solute solvation is under investigation. Apart from the solubilizing milieu, η_μ experienced by a solute also depends on the chemical structure of the solute. The interactions within the solute cybotactic region between the solute and the solvent, in turn, govern η_μ sensed by the solute. There are many solvatochromic η_μ probes whose spectral responses alter considerably with the viscosity of the cybotactic region.[35] Among such probes, fluorescence-based probes are perhaps the most used.[35,36] Probes of bifluorophoric nature containing two identical fluorophores linked by a short flexible chain that form an intramolecular excimer are found suitable to investigate η_μ of liquids and liquid mixtures.[13c,37] One of the most used fluorescence probes of this kind is BPP.[6b,38] It is well-established that in addition to the usual structured monomer fluorescence band from the pyrenyl group, a spectrally broad and unstructured emission showing a maximal intensity near 450−500 nm will also be observed, depending on the viscosity of the medium as a result of intramolecular excimer formation. For ([bmim][PF_6] + PEG) mixtures that possess relatively high viscosities, one may assume the dissociation rate of the intramolecular excimer to be slow with respect to the deexcitation, and the η_μ sensed by BPP at a given temperature can be expressed as[13]

$$\eta_\mu = \text{constant}\left(\frac{I_M}{I_E}\right)\tau_E \qquad (4)$$

where (I_M/I_E) is the BPP monomer-to-excimer emission intensity ratio and τ_E is the excimer fluorescence lifetime. Expressly, as the local viscosity increases, intramolecular association between the two pyrene units slows, resulting in a marked increase in (I_M/I_E)τ_E.

(I_M/I_E) and τ_E for BPP are experimentally obtained for all four ([bmim][PF_6] + PEG) mixtures at various temperatures

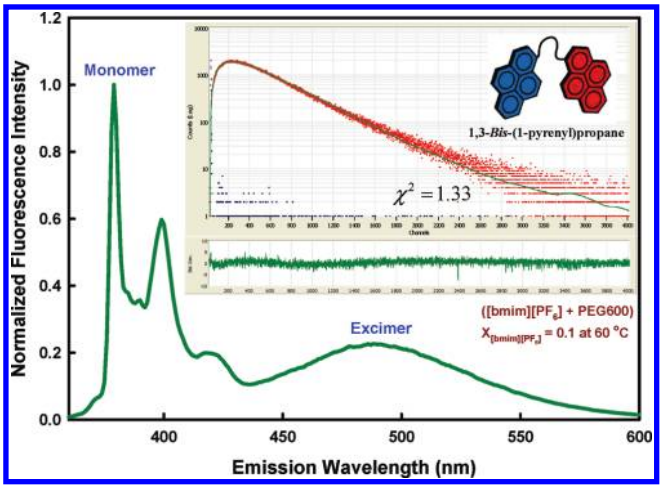

Figure 4. Steady-state fluorescence emission spectrum [$\lambda_{excitation}$ = 340 nm (Xe arc lamp),; excitation and emission slits are 1 and 1 nm, respectively] and excited-state intensity decay data [excited using 340 nm nano-LED, $\lambda_{emission}$ = 487 nm] of 1,3-bis(1-pyrenyl)propane (BPP, 10 μM) within the ([bmim][PF_6] + PEG600) mixture at 60 °C.

(an example is shown in Figure 4), and the product of the two, which is proportional to η_μ (eq 4), is plotted against $X_{[bmim][PF_6]}$ in Figure 5. A careful examination of Figure 5 reveals a very interesting outcome. While the dynamic viscosity was observed to show synergistic effect only for mixtures of [bmim][PF_6] with PEG1000 and PEG600 (Figure 1), the BPP-reported η_μ shows synergism in all four ([bmim][PF_6] + PEG) mixtures. Clearly, η_μ reported by BPP is not a reflection of the bulk viscosity of ([bmim][PF_6] + PEG400) and ([bmim][PF_6] + PEG200), mixtures containing PEGs of lower average MW. Plots of $(\ln[(I_M/I_E)\tau_E])^E$ versus $X_{[bmim][PF_6]}$ (Figure S2, Supporting Information) show that $(\ln[(I_M/I_E)\tau_E])^E$ is always positive, irrespective of the composition or the temperature of the mixture. It is noteworthy that, in general, $(\ln[(I_M/I_E)\tau_E])^E$ decreases with increasing T of the mixture, which proposes that H-bonding might be the reason for the observed synergism in η_μ within all four mixtures.

To find the reason for the difference between the bulk viscosity (η) and the BPP-reported microviscosity (η_μ) of [bmim][PF_6] mixtures with PEG400 and PEG200, respectively, it is essential to realize that the response of a η_μ probe may not be the same in two media of identical η but of different chemical nature. It was shown earlier that η_μ by a similar probe in (ethanol + glycerol) mixtures and in (hexadecane + paraffin) mixtures at 25 °C are significantly different for the mixtures with the same η.[13a,39] This is explained in terms of internal rotation involved in intramolecular excimer formation, which depends on the nature of the interactions present within the milieu. The medium participates in this internal rotation not only by the viscous drag but also by its microstructure, which depends on the interactions present within the system involving the probe.

In order to assess the effect of interactions present within neat [bmim][PF_6] as compared to the interactions present within neat PEGs of different average MW upon BPP fluorescence response, we plotted (I_M/I_E)τ_E against the corresponding η for these systems in Figure 6. It is interesting to note that for identical η, the BPP-reported η_μ decreases in the order PEG200 > PEG400 > PEG600 > [bmim][PF_6] > PEG1000. Clearly, the interactions within BPP solution of PEG200 result in the highest η_μ reported

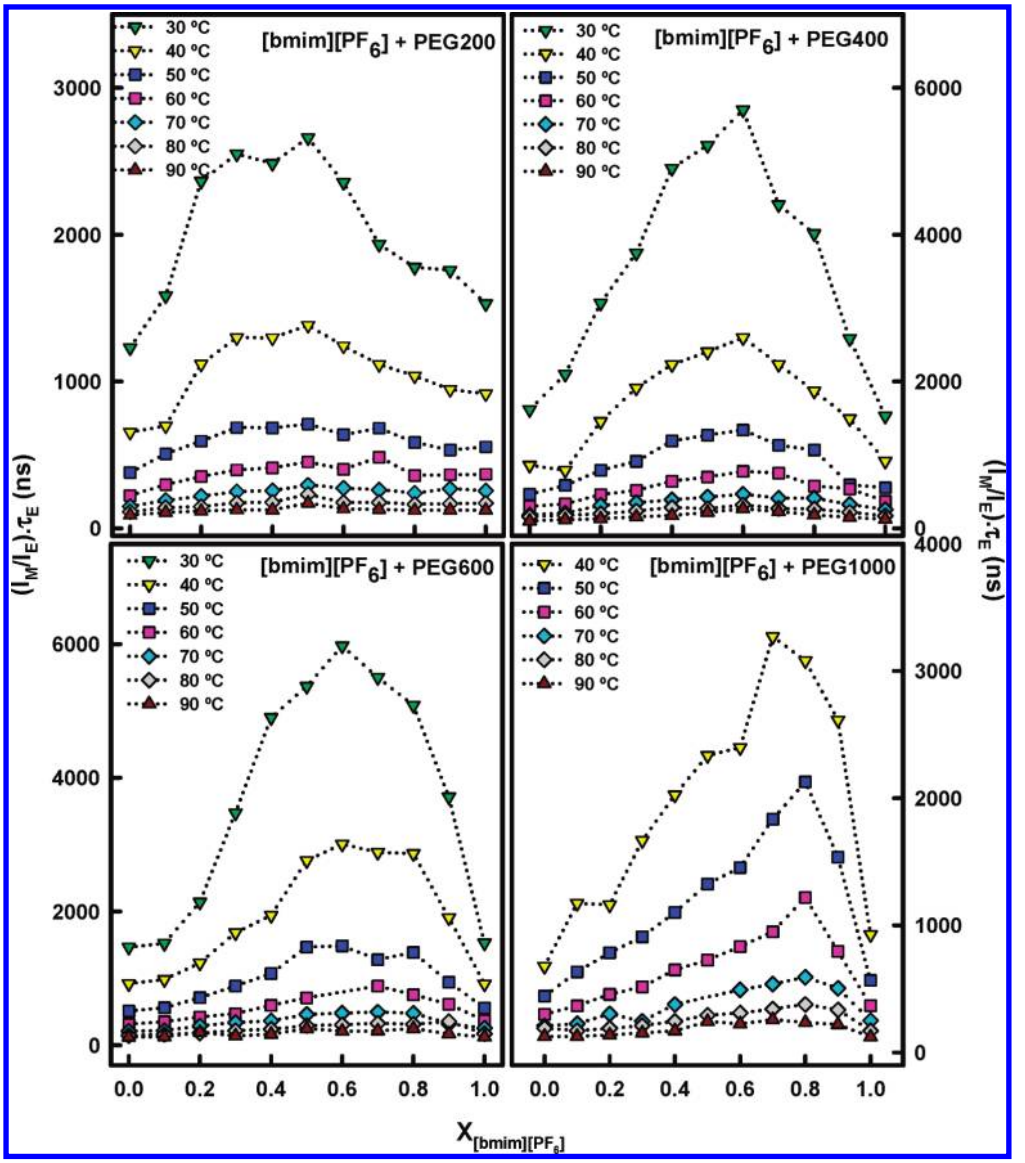

Figure 5. Product of the monomer-to-excimer fluorescence intensity ratio and the excimer fluorescence lifetime $[(I_M/I_E) \times \tau_E]$ of BPP representing microviscosity versus $X_{[bmim][PF_6]}$ for ([bmim][PF_6] + PEG) mixtures at different temperatures. Dotted curves are to guide the eyes.

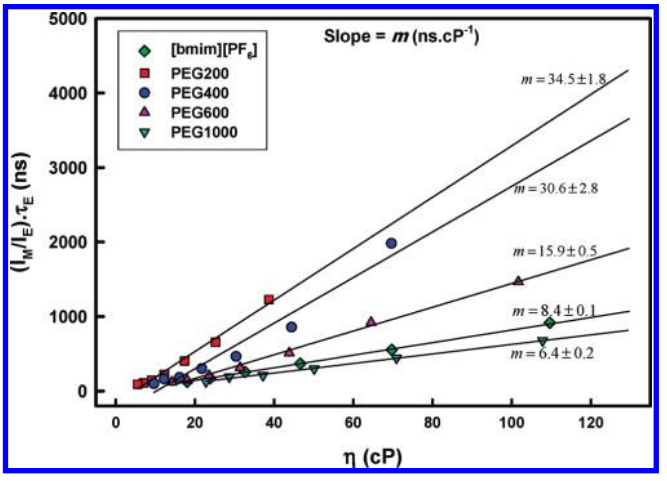

Figure 6. $[(I_M/I_E)\tau_E]$ versus η for neat [bmim][PF_6], PEG200, PEG400, PEG600, and PEG1000.

by this probe among the four neat liquids. These outcomes lead us to the dominant role of H-bonding interactions, specifically, the intermolecular type involving terminal −OH, as the major contributor toward BPP-reported η_μ. It appears that in neat [bmim][PF_6] the contribution to η from Coulombic and other non-H-bonding interactions is major, and that from H-bonding, especially between the C2−H of $bmim^+$ and PF_6^-, is minor. Further, in PEG1000, though the H-bonding interactions are present, the non-H-bonding interactions (i.e., the van der Waals type) are the major contributors to η due to a relatively longer polymer chain. Within systems where an extensive H-bonded network is present, the BPP η_μ is observed to be higher as the internal rotation within BPP to form the excimer is interfered with more by the H-bonding in comparison to the lower hindrance afforded to the excimer formation by the non-H-bonding interactions; however, the combined contribution from the H-bonding and the non-H-bonding is the same, giving rise to identical η for the two systems. Consequently, though the η of neat PEG200,

dx.doi.org/10.1021/jp203079p |J. Phys. Chem. B 2011, 115, 7405–7416

PEG400, and PEG600 are lower than that of neat [bmim][PF_6] at all temperatures, the BPP-reported η_μ of these three PEGs are similar to that of [bmim][PF_6]. This is attributed to the H-bonding being the major contributor to η of these three PEGs.

As PEG is added to [bmim][PF_6], both Coulombic and non-H-bonding interactions as well as H-bonding between $bmim^+$ and PF_6^- are replaced by H-bonding interactions between $bmim^+$ and/or PF_6^- of the IL and terminal −OH of PEG. Within [bmim][PF_6] mixtures with PEG200 and PEG400, respectively, dramatic loss in columbic attractive interactions results in lowered η; however, the formation of extensive interparticle H-bonding results in increased η_μ. A similar formation of an extensive H-bonding network between $bmim^+/PF_6^-$ and terminal −OH of PEG600 and PEG1000 results in an increase in both η and η_μ of ([bmim][PF_6] + PEG600) and ([bmim][PF_6] + PEG1000) mixtures. A complex interplay of inter- and intraparticle H-bonding versus non-H-bonding interactions decides trends in η and η_μ within ([bmim][PF_6] + PEG) mixtures. The evidence for the presence of interparticle H-bonding involving C2−H of $bmim^+$ and terminal −OH of PEG within ([bmim][PF_6] + PEG) mixtures is also provided by the FTIR absorbance data (vide supra).

CONCLUSIONS

A relatively high η of IL [bmim][PF_6] is due, in major part, to the presence of strong Coulombic attractive interactions; H-bonding between the C2−H of $bmim^+$ and PF_6^- is the minor contributor to η. The η of PEG1000 is comparable to that of [bmim][PF_6] because of the van der Waals interactions involving long polymer chains; the H-bonding involving −OH also contributes to η, though it is a minor contributor. Lower average MW PEGs have lower η as the van der Waals interactions are not as dominant due to the shorter polymer chains; contribution from H-bonding toward η is more substantial. Synergism in η is observed because of the formation of extensive H-bonding between $bmim^+$ and terminal −OH of PEG600/PEG1000 that more than compensates for the losses in Coulombic attractive interactions and van der Waals interactions within [bmim][PF_6] and PEG600/PEG1000 along with any loss of H-bonding within [bmim][PF_6] and PEG600 or PEG1000. This compensation is not enough to result in synergism in η within ([bmim][PF_6] + PEG200) and ([bmim][PF_6] + PEG400) mixtures. The BPP-reported η_μ, however, shows significant synergism in all four ([bmim][PF_6] + PEG) mixtures. The η_μ obtained using intramolecular excimer fluorescence of BPP is affected more by the H-bonding and less by the non-H-bonding interactions. Formation of a stronger and more efficient H-bonding network between the terminal −OH of PEG and the C2−H of $bmim^+$ results in synergistic η_μ even in ([bmim][PF_6] + PEG200) and ([bmim][PF_6] + PEG400) mixtures. Probe-reported η_μ in combination with bulk dynamic η highlights the importance of different interactions present within ([bmim][PF_6] + PEG) mixtures. The role of inter- and intraparticle H-bonding as well as Coulombic and van der Waals interactions on bulk dynamic viscosity and probe-reported microviscosity is amply demonstrated.

ASSOCIATED CONTENT

Supporting Information. Additional plots and FTIR absorbance results. This material is available free of charge via the Internet at http://pubs.acs.org.

AUTHOR INFORMATION

Corresponding Author

*E−mail: sipandey@chemistry.iitd.ac.in. Phone: +91−11−26596503. Fax: +91−11−26581102.

ACKNOWLEDGMENT

This work is generously supported by the Department of Science and Technology (DST), Government of India, through a grant to S.P. [Grant Number SR/S1/PC-16/2008]. S.T. would like to thank UGC, Government of India. for her fellowship.

REFERENCES

(1) (a) Ficke, L. E.; Brennecke., J. F. *J. Phys. Chem. B* **2010**, *114*, 10496. (b) Rogers, R. D.; Seddon, K. R. *Science* **2003**, *302*, 792. (c) Welton, T. *Chem. Rev.* **1999**, *99*, 2071. (d) Pandey, S. *Anal. Chim. Acta* **2006**, *556*, 38. (e) Wilkes, J. S. *Green Chem.* **2002**, *4*, 73. (f) Rogers, R. D., Seddon, K. R., Eds. *Ionic Liquids: Industrial Applications for Green Chemistry*; ACS Symposium Series 818; American Chemical Society: Washington, DC, 2002.

(2) (a) Rogers, R. D.; Seddon, K. R., Eds. *Ionic Liquids as Green Solvents: Progress and Prospects*; ACS Symposium Series 856; American Chemical Society: Washington, DC, 2003. (b) Earle, M. J.; Seddon, K. R. *Pure Appl. Chem.* **2000**, *72*, 1391. (c) Clark, J. H. *Green Chem.* **1999**, *1*, 1. (d) Leininger, N. F.; Clontz, R.; Gainer, J. L.; Kirwan, D. J. *Chem. Eng. Commun.* **2003**, *190*, 431. (e) Sherman, J.; Chin, B.; Huibers, P. D.; Garcia-Valls, R.; Hattan, T. A. *Environ. Health Perspect.* **1998**, *106*, 253. (f) Brennecke, J. F.; Stadtherr, M. A. *Comput. Chem. Eng.* **2002**, *26*, 307. (g) Tundo, P.; Anastas, P. T., Eds. *Green Chemistry: Challenging Perspectives*; Oxford Science: Oxford, U.K., 1999. (h) Noble, D. *Anal. Chem.* **1993**, *65*, 693A. (i) Anastas, P. T. In *Clean solvents, Alternative media for chemical reactions and processing*; Abraham, M. A., Moens, L., Eds.; ACS Symposium Serious 819; American Chemical Society: Washington, DC, 2002; p 1.

(3) (a) Wasserscheid, P.; Keim, W. *Angew. Chem., Int. Ed.* **2000**, *39*, 3772. (b) Sheldon, R. *Chem. Commun.* **2001**, *23*, 2399. (c) Lee, J. S.; Luo, H.; Baker, G. A.; Dai, S. *Chem. Mater.* **2009**, *21*, 4756. (d) Cocalia, V. A.; Gutowski, K. E.; Rogers, R. D. *Coord. Chem. Rev.* **2006**, *250*, 755. (e) Dominguez de Maria, P. *Angew. Chem.* **2008**, *47*, 6960. (f) Polyakova, Y.; Koo, Y. M.; Row, K. H. *Rev. Anal. Chem.* **2007**, *26*, 77. (g) Murugesan, S.; Linhardt, R. J. *Curr. Org. Synth.* **2005**, *2*, 437. (h) Behera, K.; Kumar, V.; Pandey, S. *ChemPhysChem* **2010**, *11*, 1044. (i) Behera, K.; Malek, N. I.; Pandey, S. *ChemPhysChem* **2009**, *10*, 3204.

(4) (a) Kumar, V.; Baker, G. A.; Pandey, S. *Chem. Commun.* **2011**, *47*, 4730. (b) Ali, M.; Kumar, V.; Pandey, S. *Chem. Commun.* **2011**, *46*, 5112. (c) Rai, R.; Baker, G. A.; Behera, K.; Mohanty, P.; Kurur, N. D.; Pandey, S. *Langmuir* **2010**, *26*, 17821. (d) Sarkar, A.; Trivedi, S.; Baker, G. A.; Pandey, S. *J. Phys. Chem. B* **2008**, *112*, 14927. (e) Sarkar, A.; Trivedi, S.; Pandey, S. *J. Phys. Chem. B* **2008**, *112*, 9042.

(5) (a) Dutta, P.; Rai, R.; Pandey, S. *J. Phys. Chem. B* **2011**, *115*, 3578. (b) Sarkar, A.; Trivedi, S.; Pandey, S. *J. Phys. Chem. B* **2009**, *113*, 7606. (c) Fletcher, K. A.; Pandey, S. *Appl. Spectrosc.* **2002**, *56*, 1498. (d) Trivedi, S.; Malek, N. I.; Behera, K.; Pandey, S. *J. Phys. Chem. B* **2010**, *114*, 8118.

(6) (a) Fletcher, K. A.; Pandey, S. *Appl. Spectrosc.* **2002**, *56*, 266. (b) Pandey, S.; Fletcher, K. A.; Baker, S. N.; Baker, G. A. *Analyst* **2004**, *129*, 569.

(7) (a) Scurto, A. M.; Aki, S. N. V. K.; Brennecke, J. F. *J. Am. Chem. Soc.* **2002**, *124*, 10276. (b) Solinas, M.; Pfaltz, A.; Cozzi, P. G.; Leitner, W. *J. Am. Chem. Soc.* **2004**, *126*, 16142. (c) Blanchard, L. A.; Hancu, D.; Beckman, E. J.; Brennecke, J. F. *Nature* **1999**, *399*, 6731.

(8) Fletcher, K. A.; Pandey, S. *J. Phys. Chem. B* **2003**, *107*, 13532.

(9) (a) Kerton, F. M. *Alternative Solvents for Green Chemistry*; Royal Society of Chemistry: Cambridge, U.K., 2009. (b) Imperato, G.; Konig, B.; Chiappe, C. *Eur. J. Org. Chem.* **2007**, *7*, 1049.

(10) (a) Singh, P.; Pandey, S. *Green Chem.* **2007**, *9*, 254. (b) Chen, J.; Spear, S. K.; Huddleston, J. G.; Rogers, R. D. *Green Chem.* **2005**, *7*, 64.
(11) (a) Harris, J. M.; Ed., Zalipsky, S. *Poly(ethylene glycol) Chemistry and Biological Applications*; ACS Symposium Series 680; American Chemical Society: Washington, DC, 1997. (b) Harris, J. M.; Ed. *Poly-(ethylene glycol) Chemistry: Biotechnical and Biomedical Applications*; Plenum: New York, 1992.
(12) (a) Cheremisinoff, N. P. *Industrial Solvents Handbook*, 2nd ed.; Marcel Dekker: New York, 2003. (b) Riddick, J. A.; Bunger, W. B.; Sakano, T. K. *Techniques of Chemistry, Vol. II, Organic Solvents: Physical Properties and Methods of Purification*; John Wiley & Sons: New York, 1986.
(13) (a) Valeur, B. *Molecular Fluorescence: Principles and Application*; Wiley-VCH: New York, 2001. (b) Turley, W. D.; Offen, H. W. *J. Phys. Chem.* **1986**, *90*, 1967. (c) Zana, R. *J. Phys. Chem. B* **1986**, *103*, 9117. (d) Miyagishi, S.; Suzuki, H.; Asakawa, T. *Langmuir* **1996**, *12*, 2900. (e) Bokobza, L. *Prog. Polym. Sci.* **1990**, *15*, 337.
(14) (a) Trivedi, S.; Pandey, S *Indian J. Chem.* **2010**, *49A*, 731. (b) Trivedi, S.; Pandey, S. *J. Chem. Eng. Data* **2011**, *56*, 2168.
(15) (a) Ninni, L.; Burd, H.; Fung, W. H.; Meirelles, A. J. A. *J. Chem. Eng. Data* **2003**, *48*, 324. (b) Han, F.; Zhang, J.; Chen, G.; Wei, X. *J. Chem. Eng. Data* **2008**, *53*, 2598. (c) Rahbari-Sisakht, M.; Taghizadeh, M.; Eliassi, A. *J. Chem. Eng. Data* **2003**, *48*, 1221.
(16) (a) Wang, J.; Zhu, A.; Zhao, Y.; Zhuo, K. *J. Solution Chem.* **2005**, *34*, 585. (b) *CRC Handbook of Chemistry and Physics*, 77th ed.; Lide, D. R., Frederikse, H. P. R., Eds; CRC Press: Boca Raton, FL, 1996−1997. (c) Dean, J. A., Ed.; *Langes Handbook of Chemistry*, 15th ed.; McGraw-Hill Professional: New York, 1998.
(17) Doolittle, A. K. *J. Appl. Phys.* **1951**, *22*, 1031.
(18) (a) de Guzman, J. *Anales soc. españ. fís. y quím.* **1913**, *11*, 353. (b) Andrade, E. N. da C. *Nature* **1930**, *125*, 309.
(19) Heintz, A.; Klasen, D.; Lehmann, J. K. *J. Solution Chem.* **2002**, *31*, 467.
(20) (a) Andrzejewska, E.; Golubska, M. P.; Stepniak, I.; Andrzejewski, M. *Polymer* **2009**, *50*, 2040. (b) Wang, J.; Zhu, A.; Zhao, Y.; Zhuo, K. *J. Solution Chem.* **2005**, *34*, 585. (c) Wang, J.; Tian, Y.; Zhao, Y.; Zhuo, K. *Green Chem.* **2003**, *5*, 618. (d) Tian, Y.; Wang, X.; Wang, J. *J. Chem. Eng. Data* **2008**, *53*, 2056. (e) Mokhtarani, B.; Sharifi, A.; Mortaheb, H. R.; Mirzaei, M.; Mafi, M.; Sadeghian, F. *J. Chem. Thermodyn.* **2009**, *41*, 1432. (f) Mokhtarani, B.; Sharifi, A.; Mortaheb, H. R.; Mirzaei, M.; Mafi, M.; Sadeghian, F. *J. Chem. Eng. Data* **2010**, *55*, 3901. (g) Andreas, K.; Dagmar, L.; Jochen, K. *J. Solution Chem.* **2002**, *31*, 467. (h) Mokhtarani, B.; Sharifi, A.; Mortaheb, H. R.; Mirzaei, M.; Mafi, M.; Sadeghian, F. *J. Chem. Thermodyn.* **2009**, *41*, 323. (i) Anouti, M.; Vigeant, A.; Jacquemin, J.; Brigouleix, C.; Lemordant, D. *J. Chem. Thermodyn.* **2010**, *42*, 834. (j) Froeba, A. P.; Wasserscheid, P.; Gerhard, D.; Kremer, H.; Leipertz, A. *J. Phys. Chem. B* **2007**, *111*, 12817. (k) Comminges, C.; Barhdadi, R.; Laurent, M.; Troupel, M. *J. Chem. Eng. Data* **2006**, *51*, 680. (l) Zarrougui, R.; Dhahbi, M.; Lemordant, D. *J. Solution Chem.* **2010**, *39*, 921. (m) Domanska, U.; Krolikowska, M. *J. Chem. Eng. Data* **2010**, *55*, 2994. (n) Fan, W.; Zhao, Q.; Sun, J.; Zhang, S. *J. Chem. Eng. Data* **2009**, *54*, 2307. (o) Kelkar, M. S.; Maginn, E. J. *J. Phys. Chem. B* **2007**, *111*, 4867. (p) Kurnia., K. A.; Mutalib, M. I. A. *J. Chem. Eng. Data* **2011**, *56*, 79. (q) Ganapatibhotla, L. V. N. R.; Zheng, J.; Roy, D.; Krishnan, S. J. *Chem. Mater.* **2010**, *22*, 6347. (r) Chen, T.; Chidambaram, M.; Liu, Z.; Smit, B.; Bell, A. T. *J. Phys. Chem. B* **2010**, *114*, 5790. (s) Khupse, N. D.; Kumar, A. *J. Solution Chem.* **2009**, *38*, 589.
(21) Redlich, O.; Kister, A. T. *Ind. Eng. Chem.* **1948**, *40*, 341.
(22) Wold, S.; Sjöstrom, M.; Eriksson, L. *PLS-regression: A Basic Tool of Chemometrics*; Chemom. Intell. Lab Syst.: The Netherlands, 2001; Vol. 58, p 109.
(23) Zhang, L. M.; Zhou, J. F. *Colloids Surf., A* **2006**, *279*, 34.
(24) (a) Ageno, M.; Frontali, C. *Proc. Natl. Acad. Sci. U.S.A.* **1967**, *57*, 856. (b) Song, S; Peng, C. *J. Dispersion Sci. Technol.* **2008**, *29*, 1367.
(25) Howard, K. S.; Mcallister, R. *AIChE J.* **1958**, *4*, 362.
(26) Schichman, S. A.; Amey, R. L. *J. Phys. Chem.* **1971**, *75*, 98.
(27) Wang, P.; Anderko, A. 14th International Conference on the Properties of Water and Steam; Kyoto, Japan, August 29−September 3, 2004.
(28) Ouerfelli, N.; Kouissi, T.; Zrelli, N.; Bouanz, M. *J. Solution Chem.* **2009**, *38*, 983.
(29) Fort, R. J.; Moore, W. R. *Trans. Faraday Soc.* **1965**, *61*, 1112.
(30) Crabtree, A. M.; OBrlen, J. F. *J. Chem. Eng. Data* **1991**, *36*, 140.
(31) Qunfang, L.; Yu-Chun, H. *Fluid Phase Equilib.* **1999**, *154*, 153.
(32) (a) Gilli, G.; Gilli, P. *The Nature of the Hydrogen Bond: Outline of a Comprehensive Hydrogen Bond Theory*: Oxford Science Publications: New York, 2009. (b) Jeffrey, G. A. *An Introduction to Hydrogen Bonding (Topics in Physical Chemistry)*; Oxford University Press: New York, 1997. (c) Grabowski, S. *Hydrogen Bonding — New Insights (Challenging and advances in Computational Chemistry and Physics)*; Springer: The Netherlands, 2011. (d) Khutoryanskiy, V. V., Staikos, G., Eds. *Hydrogen-Bonded Intermolecular Complexes: Formation, Structure and Applications*; World Scientific: River Edge, NJ, 2009. (e) Schuster, P.; Zundel, G.; Sandorfy, C., Eds. *The Hydrogen Bond: Recent Development in Theory and Experiments*; North-Holland Publishing Company: Amsterdam, The Netherlands, 1976.
(33) Tan., R.; He, Y.; Zhu, Y.; Xu, B.; Cao, L. *J. Mater. Sci.* **2003**, *38*, 3973.
(34) Talaty, E. R.; Raja, S.; Storhaug, V. J.; Dölle, A.; Carper, W. R. *J. Phys. Chem. B* **2004**, *108*, 13177.
(35) Lakowicz, J. R. *Principles of Fluorescence Spectroscopy*, 3rd ed.; Kluwer Academics/Plenum Publishers: New York, 2006.
(36) (a) Acree, W. E., Jr. *Absorption and Luminescence Probes. In Encyclopedia of Analytical Chemistry: Theory and Instrumentation*; Meyer, R. A., Ed.; John Wiley & Sons, Ltd.: Chichester, U.K., 2000; and references cited therein. (b) Turro, N. J. *Modern Molecular Photochemistry*; University Science Books: Sausalito, CA, 1991. (c) Gore, M. G. *Spectrophotometry and Spectrofluorimetry*; Oxford University Press: London, 2000. (d) Birks, J. B. *Photophysics of Aromatic Molecules*; Wiley-Interscience: New York, 1970.
(37) Macanita, A. L.; Zachariasse, K. A. *J. Phys. Chem. A* **2011**, *115*, 3183.
(38) (a) Fletcher, K. A.; Pandey, S. *Langmuir* **2004**, *20*, 33. (b) Fletcher, K. A.; Storey, I. A.; Hendricks, A. E.; Pandey, S.; Pandey, S. *Green Chem.* **2001**, *3*, 210. (c) Fletcher, K. A.; Pandey, S.; Storey, I. A.; Hendricks, A. E.; Pandey, S. *Anal. Chim. Acta* **2002**, *453*, 89. (d) Behera, K.; Pandey, S. J. *Colloid Interface Sci.* **2007**, *316*, 803. (e) Behera, K.; Pandey, S. *J. Phys. Chem. B* **2007**, *1*, 13307. (f) Behera, K.; Pandey, S. *Langmuir* **2008**, *24*, 6462.
(39) Viriot, M. L.; Bouchy, M; Donner, M.; Andre, J.-C. *Photochem. Photobiophys.* **1983**, *5*, 293.